A MAGNETICALLY ENHANCED WIRELESS MICRO-GEIGER COUNTER

Christine K. Eun[1], Ranjit Gharpurey[2] and Yogesh B. Gianchandani[1]
[1]*Department of Electrical Engineering and Computer Science, University of Michigan, Ann Arbor*
[2]*Department of Electrical and Computer Engineering, University of Texas, Austin*

ABSTRACT

This paper reports a micromachined Geiger counter with integrated permanent magnets that enhance the RF transmission from the discharges initiated by incident beta particles. With the intent of wireless sensing within the ultra wideband (UWB) spectrum, the transmission in the 2.0-2.8 GHz frequency range is investigated. The device consists of a 1x2 cm^2 micromachined glass/Si cavity sandwiched between two miniaturized NdFeB rare earth magnets. Several different magnet orientations as well as two different shapes of magnets (square and ring) are investigated. The square and ring magnets have a maximum flux density of 2.40 and 0.91 kG, respectively. Preliminary results show that the RF spectra in the presence of ^{90}Sr and ^{204}Tl sources of 0.1-1.0 μCi increased by ~8 relative dBμV (compared to non-magnetic devices) at a distance of 5 cm from the device. The radiation pattern emitted by the microdischarges is measured in the plane of the device. Wireless spectra from electrostatic discharges are also reported.

I. INTRODUCTION

Past work on lithographically microfabricated radiation sensors has included solid-state and gas-based X-ray detectors [1-5]. It has been shown that a micromachined Geiger counter generating gas microdischarges created by the passage of a beta particle transmits radio-wave signals potentially suitable for sensor networking [6,7]. These RF transmissions produced by the microGeiger were controlled by bias circuitry components.

Gas discharges across relatively large gaps (on the order of cm) have been employed in the past with spark gap transmitters for communication applications dating back to Guglielmo Marconi in the mid-1890's [8]. In 1901, Bose reported utilizing discharges within waveguides in order to generate microwaves, and more recent activity has also been reported [9].

Networked radiation sensors are envisioned for monitoring public buildings with high pedestrian traffic such as train stations, football stadiums and shopping malls. Wireless communication between sensors can enable rapid and low cost deployment or reconfiguration of networks. Wireless networks can also be employed for monitoring environmental hazards and inaccessible terrains. The prospect of not only utilizing the inherent RF transmissions from discharge-based sensors, but also to have the ability to control and influence the wireless signal output is very attractive from a viewpoint of implementing a wireless network.

Employing large permanent magnets in plasma magnetron systems for micromachining have found widespread use with sputtering deposition systems. Traditionally, plasma magnetrons made use of powerful magnets to increase plasma density and consequently increase sputtering efficiency. The mean free path is relatively large (on the order of a few cm) due to operation at lower pressures (on the order of 5-10 mTorr of pressure) [10]. Miniaturized permanent magnets have been utilized in the past to enhance and confine dc microplasmas to enable localized, maskless etching of silicon with SF_6 gas [11].

This paper presents a magnetically enhanced micromachined Geiger counter for β-particle detection, which uses permanent magnets along with glass/Si structures to produce wireless transmission in the ultra wideband (UWB) window. In Section II, device concepts such as basic wireless Geiger operation as well as the magnet configuration used to achieve RF field strength enhancement is discussed. Section III presents the recent experimental results including field enhancement data and emission pattern plots. Section IV concludes with a discussion of possible applications.

II. DEVICE CONCEPTS AND OPERATION

Basic Wireless Geiger Operation

The basic device includes a lithographically micromachined component which is a glass-Si-glass sandwich in which a central Si post forms the cathode and a peripheral Si ring forms the anode. This component measures 1x2 cm^2 and contains 6 different detection cavities that share a common anode on each die. The region proximal to the cathode has a weak field and is called the drift region, whereas that adjacent to the anode is the higher field amplification region. Discharges can be either electrostatically initiated (exceeding gas breakdown voltage) or beta particle-initiated. As beta particles pass through the glass window, they ionize the surrounding gas atoms, resulting in an avalanche current pulse and consequent RF transmission. The micro-Geiger device inherently operates as a UWB transmitter along the guidelines specified in [12].

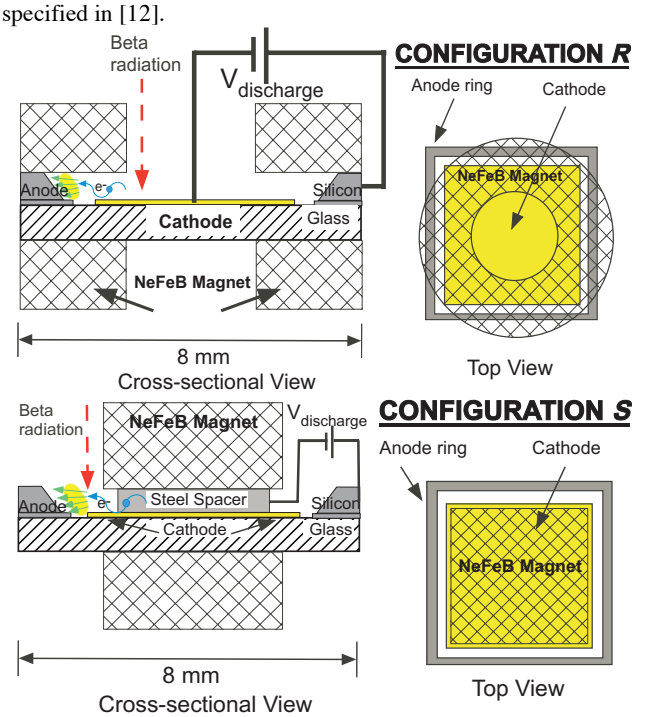

Fig. 1: (a) Cross-section of device in ring magnet configuration (Configuration *R*). (b) Cross-section of device in square magnet configuration (Configuration *S*).

Magnetic Enhancement Configuration

Configuration *R* (Fig. 1a) and Configuration *S* (Fig. 1b) show the cross-section of the device in the different configurations tested.

They utilize strong magnetic fields provided by miniaturized neodymium-iron-boron (NdFeB) rare earth magnets. Ring-shaped as well as square-shaped magnets were used to construct the sandwich structures. Each square magnet measured 6x6x6 mm^3. A steel spacer was utilized as the cathode electrode contact to avoid passing large amounts of current through the permanent magnets and consequently damaging the upper permanent magnet. Each ring magnet measured 6 mm outer radius and a 2.5 mm inner radius. Figure 2 shows a photograph of the micro-Geiger device assembled in Configuration *R*. The electrical contact for the cathode passes through the opening of the top ring-shaped magnet. The structure is stabilized by the second magnet located below the micromachined Geiger counter. The magnetic field lines were aimed to be positioned perpendicular to the discharge path.

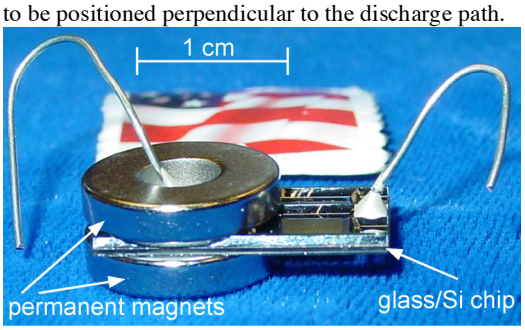

Fig. 2: Photograph of micro-Geiger device in the ring magnet arrangement (Configuration *R*).

A particle that is moving in the presence of both an electric field and an orthogonal magnetic field, B_0, which is also consequently perpendicular to the discharge path, will give rise to a drift velocity, v_F, perpendicular to both fields:

$$v_F = \frac{(\mathbf{F}_\perp / q) \times \mathbf{B}}{B_0^2} \qquad (1)$$

$F_\perp$ represents the transverse force due to the electric field acting on the particle. **B** is the component of the magnetic field that is orthogonal to the electric field and *q* represents the charge. The particle velocity is directly proportional to the applied magnetic field. The particle will experience a gyrating motion, much like a spiral coil course, around this new, elongated discharge path [13]. Since each accelerating particle emits electromagnetic radiation, increasing the number of excited atoms can generate a stronger overall signal. In essence, this new discharge path provides an opportunity for more ion-to-neutral gas atom collisions and thereby creates more ionized particles that can participate in the wireless transmission.

III. EXPERIMENTAL RESULTS

Magnetic field strength measurements of each magnet (square and ring) were taken in the X and Z direction with a Hall sensor and the results are shown in Fig. 3a and Fig. 3b, respectively. The magnetic flux density in the Z direction of each square magnet ranged from 0.17 to 2.40 kG measured at a distance from 2 to 12 mm. The strength of the ring magnet in the Z direction varied from a flux density of 0.11 to 0.91 kG measured at a distance of 3 to 16 mm. In the X direction, the strength varied between 0.05 to 0.50 kG and 0.05 to 0.90 kG for the square and ring magnet, respectively. The X distances ranged between 5 to 21 mm. The strength of the square magnet in the Z direction was greater than the ring magnet but was measured to be weaker in the X direction. The measured magnetic field strength dropped off exponentially as expected.

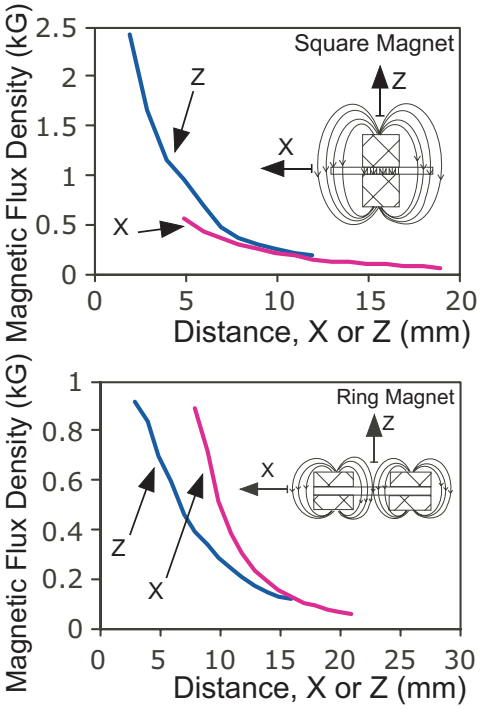

Fig. 3: (a) Magnetic flux density of a square magnet with respect to axial distance measured with a Hall probe (Bell Hall Generator: BH-205). (b) Magnetic flux density of a ring magnet with respect to axial distance.

The antenna of an RF field strength analyzer was positioned 91.5 cm away from the device while the source to detector distance was fixed at 5 cm. Frequency scans were taken in narrow-band frequency modulation (NBFM) reception mode spanning the frequency range from 2.0 GHz to 2.8 GHz in 5 MHz steps. All measurements were taken in a Ne/air gas environment with the various magnetic arrangements summarized in Table I. (A compass was used to determine the pole direction on the magnet.) For beta-initiated discharges, the pure beta emitters, ^{90}Sr and ^{204}Tl, were used with strengths 0.1 and 1.0 μCi, respectively.

Figure 4 shows the resulting spectrum using the square magnet assembly (Configuration *S*) during electrostatic breakdown. Electrostatic breakdown occurs when the applied voltage exceeds the gas breakdown potential. A significant increase in signal strength (~7 rel. dBμV) was observed around 2.3 and 2.6 GHz compared to the control measurement. The control measurement for Configuration *S* was taken without magnets present but with the steel spacer providing electrical contact to the cathode. Figure 5 shows the same configuration but this time with beta-initiated discharges using the radioisotope, ^{204}Tl. The resulting spectra showed a dramatic improvement in field strength (~8 dBμV) between 2.0 and 2.8 GHz with the exception of 2.2 to 2.3 GHz.

Table I: Magnet shape and pole orientation for each configuration.

Configuration	Magnet shape	Pole orientation
SN	Square	North up
SS	Square	South up
RN	Ring	North up
RS	Ring	South up

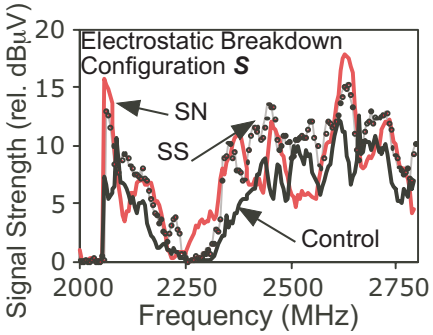

Fig. 4: Discharge spectra of electrostatic breakdown measured using an RF field strength analyzer (Protek, Inc., #3290). The control was taken in the absence of magnets with steel spacer providing electrical contact to cathode. Configuration *SN* and *SS* are also shown. Spectral strength increases in the presence of the magnetic field. Tests were conducted in a Ne/air environment.

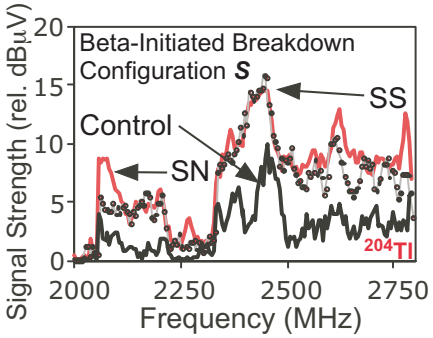

Fig. 5: Discharge spectra of beta-initiated breakdown using ^{204}Tl as the radioactive source. Configuration *SN* and *SS* are shown along with the control measurement.

Figures 6 and 7 illustrate the same series of measurements but this time using the dual ring-shaped assemblage (Configuration *R*). Both plots show significant increase in signal strength measured when compared to the control measurement. Figure 8 compares the resulting spectra when the electrode roles are reversed (anode becomes cathode, cathode becomes anode): this decreased spectral strength.

A measurement was performed to determine the directionality of the transmitted RF spectra. The experimental set-up is illustrated in Fig. 9, whereas the emitted radiation pattern of the RF transmissions from the microdischarges received as a function of in-plane rotation angle has been plotted in Fig. 10. The applied bias voltage was kept constant at 900 V in the presence of ^{90}Sr while the sensor and source were rotated at various angles relative to the RF field strength analyzer. Figure 10(a-top) shows the control measurement of the RF transmission characteristics in the absence of the permanent magnets spanning from 0° to 180°, measured at 15° intervals, at a constant radius of 91.5 cm. The tested frequencies spanned 2.0 to 2.8 GHz in NBFM reception mode. Electrical contact was made directly to the central cathode. The plot shows fairly uniform spectra spanning the perimeter of the circle. Figure 10(b-bottom) shows the same transmission characteristics, this time in the presence of the applied magnetic field in Configuration *RN*. A fairly uniform enhancement in the spectrum in the presence of the magnets compared to the absence was observed.

These results show a clear magnetic enhancement of spectral strength observed while operating in both Configuration *S* and Configuration *R*. Experimental results have also demonstrated that the microdischarges are relatively uniform and thereby independent of rotation angle. This supports the idea that magnetic enhancement of the RF transmission is taking place rather than magnetic shaping of the spectra.

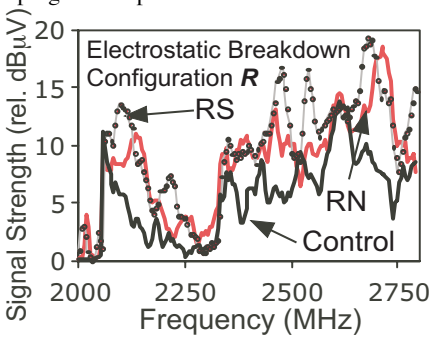

Fig. 6: Discharge spectra of electrostatic breakdown. The control was taken in the absence of magnets. Configuration *RN* and *RS* are also shown. A significant peak increases in signal strength can be seen around 2.1, 2.5 and 2.7 GHz.

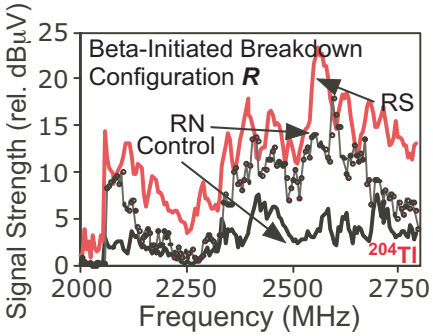

Fig. 7: Discharge spectra of beta-initiated breakdown using ^{204}Tl as the radioactive source. Significant spectral enhancement was achieved spanning the entire 800 MHz (2.0-2.8 GHz) bandwidth in the presence of the magnetic field.

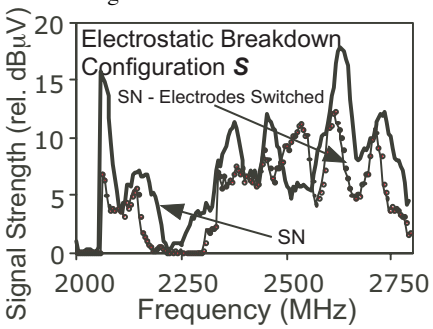

Fig. 8: Discharge spectra of electrostatic breakdown. Electrodes were switched (anode became cathode, cathode became anode) with Configuration *SN*. Switching of electrodes decreased the spectral strength measured.

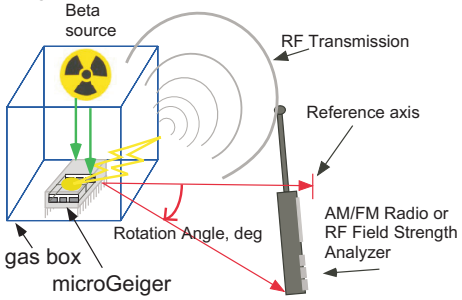

Fig. 9: Schematic illustrating rotation angle used to plot radiation pattern. The reference axis defined the 0° measurement and all subsequent angles were measured from this. Measurements ranged from 0° to 180° in 15° intervals.

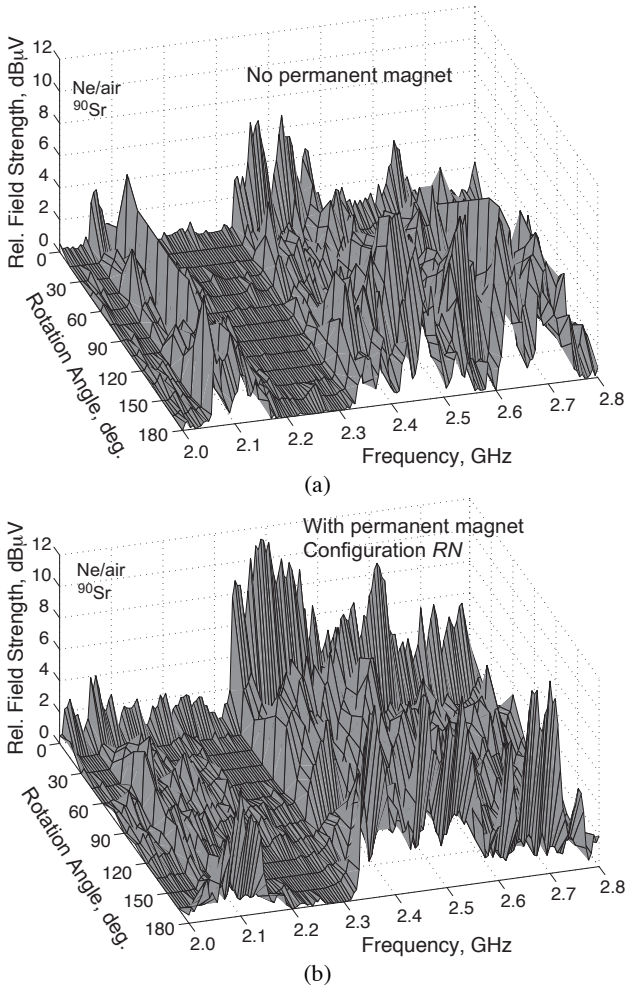

Fig. 10: Radiation pattern plots for the microGeiger discharges spanning from 0° to 180° around the perimeter of a circle with a radius of 91.4 cm. (a-top) Taken in the absence of an external magnetic field. (b-bottom) Taken in the presence of an external magnetic field, Configuration *RN*. The 2.0-2.8 GHz radiation patterns are fairly uniform around the circle.

IV. CONCLUSIONS

With the fast emergence of wireless sensor applications along with new wireless standards, developing distributed wireless sensing networks is very attractive. Utilizing miniaturized magnets to considerably increase the inherent emission characteristics of discharge-based transducers that do not require additional electronics would be a significant step in wireless sensor networking. The presence of the magnetic field induces a drift velocity of the electrons and ions that is perpendicular to the discharge path. This additional velocity force results in a change in the current discharge behavior that is realized during operation of the microGeiger. The device integrated a 1x2 cm^2 micromachined glass/Si cavity between two miniaturized NdFeB rare earth magnets. Experiments involved several different magnet orientations as well as two different shapes of magnets (square and ring) were investigated. Weak radioactive sources with strengths ranging from 0.1-1.0 μCi were used. Each square and ring magnet had a maximum flux density of 2.40 and 0.91 kG, respectively. Preliminary results show that in the presence of miniaturized magnets, the RF spectra emitted by the gas discharges in the 2.0 to 2.8 GHz frequency range showed consistent increase in the field strength intensity. The significant change in the received RF spectrum shows the influence of the magnets on the plasma resistance even at atmospheric pressure. Increasing field strength can offer a larger transmission distances and a potentially wider sensing area. Experimental results have also demonstrated that the microdischarges are relatively independent of rotation angle.

It is noteworthy that discharges are observed in other contexts in the micro-domain. Microdischarge-based chemical sensors used for vapor and liquids are known to produce optical spectra that are characteristic of chemical species [14]. Additionally, microdischarges are generated unintentionally in electrostatic transducers [15]. The findings presented here could potentially extend to these other contexts.

ACKNOWLEDGEMENTS

This work was supported primarily by the Engineering Research Centers Program of the National Science Foundation under Award Number EEC-9986866. The facilities used for this research include the Michigan Nanofabrication Facility (MNF) at the University of Michigan. The authors would like to thank Tze-Ching (Richard) Fung for his assistance with the test setup and measurement advice in this effort.

REFERENCES

[1] S. A. Audet, E. M. Schooneveld, S. E. Wouters and M. H. Kim, "High-Purity Silicon Soft X-Ray Imaging Sensor," *Sensors and Actuators*, (A22), nos. 1-3, Mar. 1990, pp. 482-486.

[2] G. Charpak, J. Derre, Y. Giomataris, P. Rebourgeard, "Micromegas, a multipurpose gaseous detector," *Nuclear Instruments & Methods in Physics Research,* (A478), nos. 1-2, Feb. 2002, pp 26-36.

[3] J. A. Kemmer, "Silicon detectors for nuclear radiation," *IEEE Transducers,* 1987 A478, pp. 252-257.

[4] M. Wada, J. Suzuki, and Y. Ozaki, "Cadmium telluride ß-ray detector," *IEEE Transducers*, 1987 A478, pp. 258-261.

[5] R. Wunstorf, "Radiation hardness of silicon detectors: current status," *IEEE Transactions on Nuclear Science,* 44(3), Jun. 1997 pp. 806-14.

[6] C. K. Eun, R. Gharpurey, and Y. B. Gianchandani, "Broadband wireless sensing of radioactive chemicals utilizing inherent RF transmissions from pulse discharges," *IEEE Intl. Conf. on Sensors*, Nov. 2005.

[7] C. K. Eun, R. Gharpurey, and Y. B. Gianchandani, "Controlling Ultra Wide Band Transmissions from a Wireless Micromachined Geiger counter," *IEEE Intl. Conf. on Micro Electro Mechanical Systems*, Jan. 2006.

[8] J. E. Brittain, "Electrical engineering Hall of Fame: Guglielmo Marconi," *Proceedings of the IEEE*, 92(9), Aug 2004, pp 1501-4.

[9] A. G. Heaton and J. H. Reeves, "Microwave radiation from discharges," *3rd Intl. Conf. on Gas Discharges*, Sept. 1974, pp 73-77.

[10] C. H. Shon, J. K. Lee, H. J. Lee, Y. Yang, and T. H. Chung, "Velocity Distributions in Magnetron Sputter," *IEEE Transactions on Plasma Science*, 26(26), Dec. 1998, pp 1635-1644.

[11] C. G. Wilson and Y. B. Gianchandani, "Miniaturized Magnetic Nitrogen DC Microplasmas", *IEEE Transactions on Plasma Science*, 32(1), Fe. 2004 pp. 282-287.

[12] FCC 02-48, First Report and Order, "Revision of Part 15 of the Commission's Rules Regarding Ultra-Wideband Transmission Systems," Feb 14, 2002: http://hraunfoss.fcc.gov/edocs_public/attachmatch/FCC-02-48A1.pdf.

[13] M. A. Lieberman and A. J. Lichtenberg, *Principles of Plasma Discharges and Materials Processing*, John Wiley and Sons, Inc. 2nd Edition,2005.

[14] B. Mitra and Y. B. Gianchandani , "The micromachined flashFET: a low-power, three-terminal device for high speed detection of vapors at atmospheric pressure,"*IEEE Intl. Conf. on Micro-Electro- Mechanical Systems*, Jan. 2005, p 794-7.

[15] T. Ono, Y. Dong, M. Esashi, "Microdischarge and electric breakdown in a micro-gap," *Journal of Micromechanics and Microengineering*, 10(3) 9/00, pp. 445-51.